PPPL Calculation Form

Calculation # CSU-CALC-132-03-0 Revision # 0 WP # 1540 (ENG-032)

Purpose of Calculation: (Define why the calculation is being performed.):

This calculation advances a simple, fast, and accurate method for calculating OOP torque loads on TF coil conductors for any poloidal field scenario, using the Excel spreadsheet that I previously distributed on 26 June 2009, which is this memo's Reference (2) document. This calculation also includes a numerical analysis of maximal loading densities for the full ranges of expected currents in the OH coil, PF coils, and plasma.

References (List any source of design information including computer program titles and revision levels.)

Reference 1: R. Woolley memo, "NSTX CSU Poloidal Fields", 26 June 2009

Reference 2: R. Woolley, Excel file NSTX_CSU_Poloidal_Field_Flux-5cm-plots.xls, issued with Ref.1 on 26 June 2009

Note: Both of these references are part of CSU-CALC-131-01-00 dated 26 June 2009.

Assumptions (Identify all assumptions made as part of this calculation.):

Algorithms advanced by this memo follow from the physics and mathematics of axisymmetric magnetic fields and from the approximating assumptions that OH and PF coil currents flow only in the toroidal direction while TF coil currents are confined to the local poloidal half-plane.

Numerical results reported in this memo are dependent also on the design point description assumed for OH and PF coils. These assumed design point detailed coil descriptions would possibly change if the NSTX CS upgrade project were to subsequently adopt a different design point.

Calculation (Calculation is either documented here or attached) - Attached (Memo: 13-260709)

Conclusion (Specify whether or not the purpose of the calculation was accomplished.):

This calculation advances a simple but precisely accurate algorithm for evaluating out-of-plane torques due to magnetic interactions of poloidal magnetic fields with TF conductor current. Instead of the conventional complicated approach involving numerical integration of vector cross products of position vectors, current density vectors and poloidal magnetic field vectors at many evaluation points chosen along a segment of the TF conductor, this algorithm simply multiplies the [(130kA)(36turn)=4680000A] TF current magnitude by the difference of the per radian poloidal magnetic fluxes evaluated at the two ends of the segment. (Note that the product of amperes and webers has the torque units, newton-meters.) The results are mathematically equivalent but the torque algorithm advanced herein requires less computation and is subject to less error. A full exposition of the torque algorithm is given in this memo's Appendix.

Cognizant Engineer's printed name, signature, and date

Robert D. Woolley Robert D Woolley Digitally signed by Robert D Woolley DN: cn=Robert D Woolley, o, ou, email=rwoolley@pppl.gov, c=US Date: 2009.08.11 14:12:37 -04'00'

I have reviewed this calculation and, to my professional satisfaction, it is properly performed and correct.

Checker's printed name, signature, and date

_____

13-260709

To: Distribution Date: 26 July 2009

From: R. Woolley Subject Out-Of-Plane (OOP) PF/TF Torques On TF Conductors in NSTX CSU

References:

1. **R. Woolley memo, "NSTX CSU Poloidal Fields", 26 June 2009**
2. **R. Woolley, Excel file NSTX_CSU_Poloidal_Field_Flux-5cm-plots.xls, issued with Ref.1 on 26 June 2009**

Summary

This memo advances a simple but precisely accurate algorithm for evaluating out-of-plane torques due to magnetic interactions of poloidal magnetic fields with TF conductor current. Instead of the conventional complicated approach involving numerical integration of vector cross products of position vectors, current density vectors and poloidal magnetic field vectors at many evaluation points chosen along a segment of the TF conductor, this algorithm simply multiplies the [(130kA)(36turn)=4680000A] TF current magnitude by the difference of the per radian poloidal magnetic fluxes evaluated at the two ends of the segment. (Note that the product of amperes and webers has the torque units, newton-meters.) The results are mathematically equivalent but the torque algorithm advanced herein requires less computation and is subject to less error. A full exposition of the torque algorithm is given in this memo's Appendix.

The algorithm is applied to the NSTX CS upgrade, using the latest layout for the TF conductor outline and using the OH/PF coil set assumed by Reference 1, in which PF1ABC coil turn numbers were 120/180/180, respectively. To increase numerical accuracy the TF conductor is partitioned into fsubregions separated by internal current streamlines estimated by equally subdividing the conductor cross section area. Torque loading densities for current ranges in each of the 13 PF and OH coil circuits and for the plasma current are plotted. MATLAB version R2008b was used for all numerical calculations and plots.

Torque Algorithm Results

Concerns have been expressed about supporting net torques on the TF outer legs by the opposing net torques on the TF central bundle and radial conductor assemblies. A simple algebraic formula is obtained from the torque algorithm for net torque on the TF outer legs, as Eq.(1):

$$\left[\frac{\text{Net TF System OuterLeg Torque}}{1\,\text{N - m}}\right] = 6315.4\left(\frac{n_{PF1AU}^{turns}}{120}\right)\left[\frac{I_{PF1AU}-I_{PF1AL}}{1\,\text{kA}}\right] + 20167.5\left(\frac{n_{PF1BU}^{turns}}{180}\right)\left[\frac{I_{PF1BU}-I_{PF1BL}}{1\,\text{kA}}\right] + 36655.0\left(\frac{n_{PF1CU}^{turns}}{180}\right)\left[\frac{I_{PF1CU}-I_{PF1CL}}{1\,\text{kA}}\right] + 12478.3\left[\frac{I_{PF2U}-I_{PF2L}}{1\,\text{kA}}\right] + 14566.9\left[\frac{I_{PF3U}-I_{PF3L}}{1\,\text{kA}}\right] \quad (1)$$

Note that vertically symmetric currents in OH, PF4 and PF5 circuits do not contribute to net TF OuterLeg torque, nor does plasma current in the vertically symmetric plasma model used herein.

Larger typical values are predicted for net torque summed over the entire top half of the TF system, including the upper half of the TF central bundle, the upper radial assemblies, and the upper half of the TF outer legs. These torques are of course balanced by opposing torques developed in the bottom half of the TF system. A formula for net torque on the top half of the TF system is as follows:

$$\begin{aligned}\left[\frac{\text{Net Upper Half TF System Torque}}{1\,\text{N-m}}\right] = 13563.1\left[\frac{I_{OH}}{1\,\text{kA}}\right] + 4240.0\left(\frac{n^{\text{turns}}_{PF1AU}}{120}\right)\left[\frac{I_{PF1AU}+I_{PF1AL}}{1\,\text{kA}}\right] \\ + 8892.5\left(\frac{n^{\text{turns}}_{PF1BU}}{180}\right)\left[\frac{I_{PF1BU}+I_{PF1BL}}{1\,\text{kA}}\right] + 16750.0\left(\frac{n^{\text{turns}}_{PF1CU}}{180}\right)\left[\frac{I_{PF1CU}+I_{PF1CL}}{1\,\text{kA}}\right] \\ + 5197.5\left[\frac{I_{PF2U}+I_{PF2L}}{1\,\text{kA}}\right] + 21915.7\left[\frac{I_{PF3U}+I_{PF3L}}{1\,\text{kA}}\right] \\ + 56813.9\left[\frac{I_{PF4}}{1\,\text{kA}}\right] + 118636.5\left[\frac{I_{PF5U}}{1\,\text{kA}}\right] + 713308.9\left[\frac{I_{plasma}}{1\,\text{MA}}\right]\end{aligned} \tag{2}$$

Similar torque formulae can be obtained for out-of-plane torques on any TF conductor circuit segment, using poloidal magnetic flux values calculated at that segment's ends. Note that the shape of the TF conductor segment between its ends is not needed to determine its net torque.

Poloidal magnetic flux can be evaluated by use of the Ref.(2) Excel spreadsheet. This tool automatically calculates poloidal flux on a grid of 5 cm (r,z) squares extending throughout the entire NSTX CSU poloidal half-plane out past its TF conductors, for any user-specified set of currents in the OH coil, PF coils, and plasma.

OOP Torque Analysis of NSTX CSU

The latest NSTX CSU TF conductor shape definition was provided by Peter Titus on 26 June 2009 in a file containing XYZ 3D coordinates of 4229 nodal points delimiting hexahedral elements in a 30 degree sector global TF model. These were subsequently culled and sorted by various automated MATLAB methods to obtain a poloidal half-plane outline consisting of 322 points, including an inner outline trace of 159 points and an outer outline trace of 163 points. These points were only modified from the provided file by setting their third coordinate values to zero without changing their other two coordinates. The resulting TF conductor outline appears in the following Fig.(1) MATLAB plot.

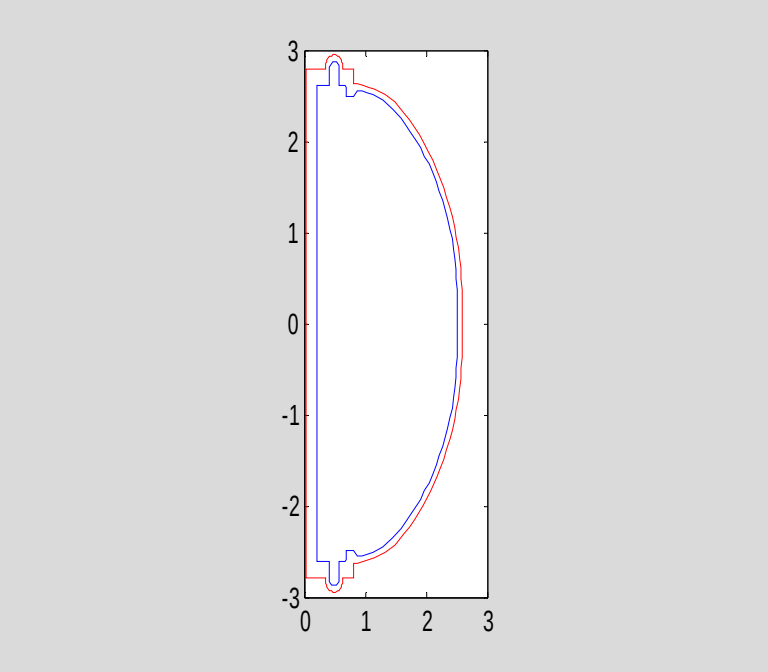

Figure 1: Poloidal Projection Outline of TF Conductor, 322 points

Parametric variables were then calculated and saved for each point in each of the two outline traces, starting from zero at their innermost points on the (z=0) horizontal midplane and adding the distances to each successive point while proceeding in the counterclockwise direction. After returning to the starting points, the saved parametric values were then normalized by dividing each cumulative distance value by its contour's total perimeter length. The resulting parametric variables, which range from 0 to 1, represent poloidal angle.

Finally, 2000 uniformly spaced values of this poloidal angle variable ranging from 0 to 1 were generated and 2000 corresponding r and z coordinate values were obtained for each of the TF coil's inner and outer outline curves by using MATLAB's standard interpolation m-files. The two resulting 2000-point outlines are plotted below in Fig. (2). Note that although they appear almost identical to the previous TF outline plot, each outline here consists of 2000 equally spaced points which are now linked to each other through their common normalized poloidal variable values.

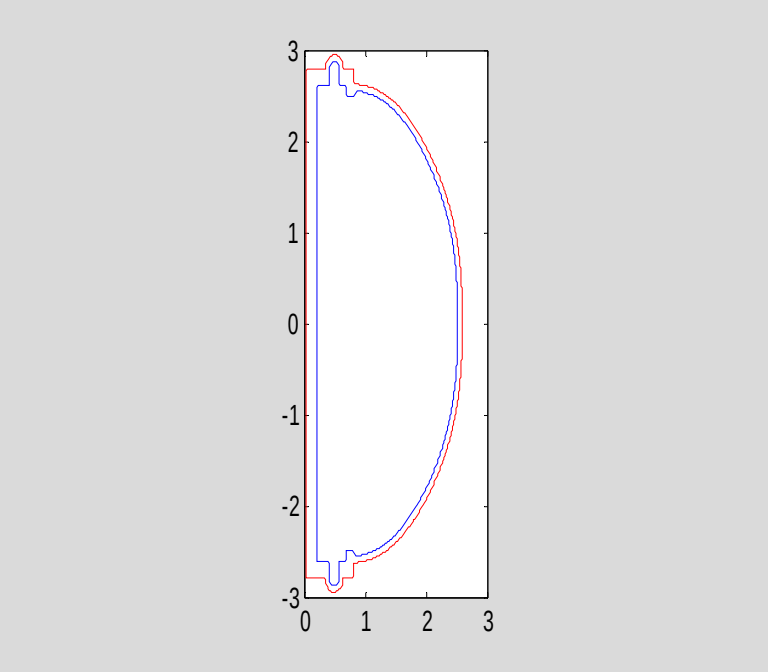

Figure 2: Poloidal Projection Outline of TF Conductor, 4000 points

Note that the TF current stream function which varies with the (r,z) location in the poloidal half-plane is defined as the total TF system current that passes through the 3D circle sharing those cylindrical coordinates. It varies from zero at (r,z) locations not linking the TF coils to the total TF current (i.e., number of turns times current per turn) at locations within the TF coil system bore. At intermediate locations within the TF conductor it varies between those values. Level set contours of the TF current stream function are also streamlines of the TF current flow.

As plotted, the (red) outer outline is the zero value contour of the TF current stream function and the (blue) inner outline is the contour of the TF current stream function at its full, 100% of TF system current, value. It was decided for calculations herein to try to improve accuracy by estimating how the TF current is distributed within the TF conductor. This was done by estimating the (r,z) coordinate locations at each of 2000 poloidal variable points for TF current stream function contours enclosing 25%, 50%, and 75%, respectively, of the total TF current. Ideally these contour estimates would be obtained by solving conductive media equations using ohms law, but this was not done. Instead, the estimated contours were obtained by interpolation between the outline coordinates for common poloidal angle variables. For the vertical (z) coordinates, linear interpolation was used directly. However, a different method was used to interpolate the r coordinate since conductor thickness in the toroidal direction varies in proportion to r for locations in and near the TF central bundle but takes on constant thickness for outer locations. Linear interpolation of a nonlinear function was used, where that function switched from a quadratic for inner locations to a straight line for outer locations. For this purpose the switchover radius between variable and constant toroidal thickness was estimated as r=0.3339 meters, based on inspection of plots showing the 4229 points of the global model.

The Fig.(3) plot follows showing the resulting estimated three internal contours and the two bounding contours of the TF current stream function.

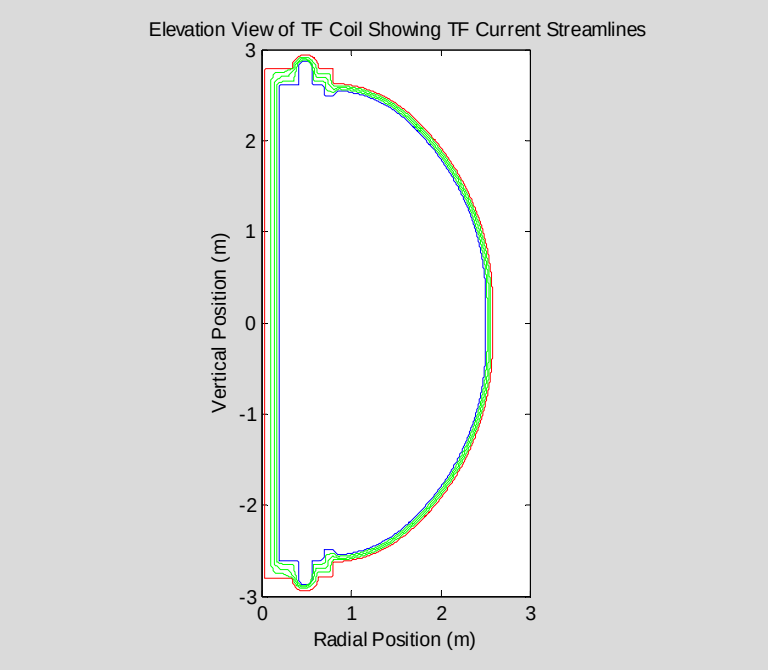

Figure 3: Poloidal Projection of TF Current Stream Function Contours, 10000 points

It may be useful to have plots showing r and z for the bounding outlines and internal contours as functions of the poloidal angle parametric variable. These follow:

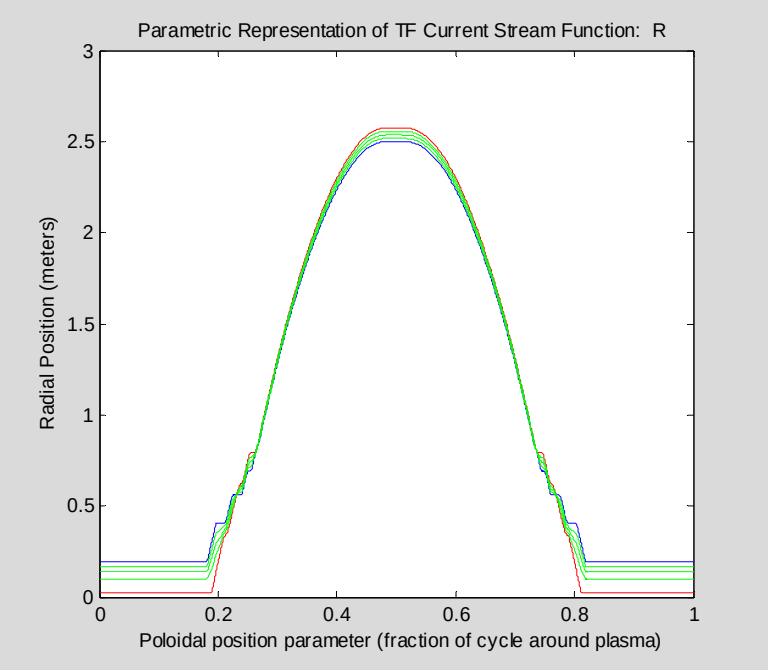

Figure 4: Radial Coordinates of TF Current Stream Function Contours vs Poloidal Variable

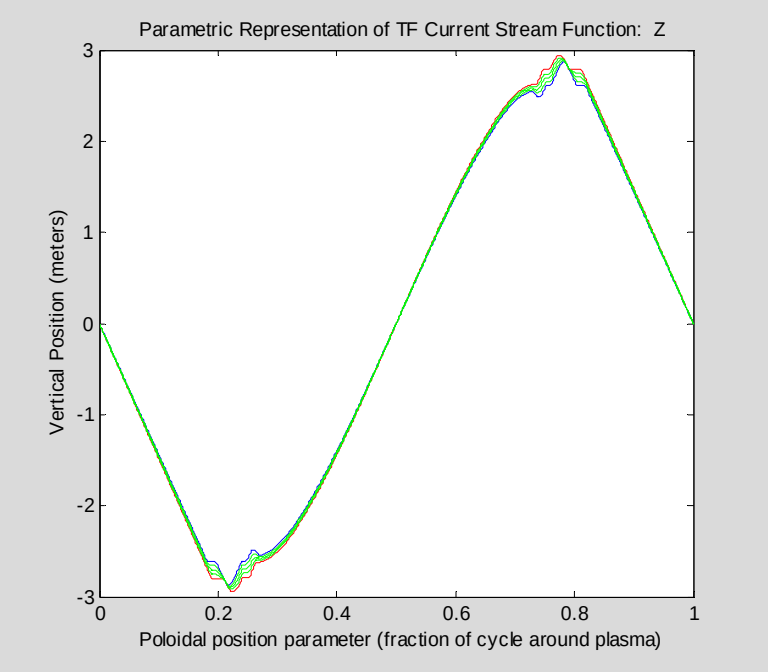

Figure 5: Vertical Coordinates of TF Current Stream Function Contours vs Poloidal Variable

In order to proceed further it is necessary to specify a PF coil set. It was decided to use the same PF coil set representation that had been used in Reference 1. Details of the assumed PF and OH coils have been reproduced here as Table 1 and are depicted in Fig.(6).

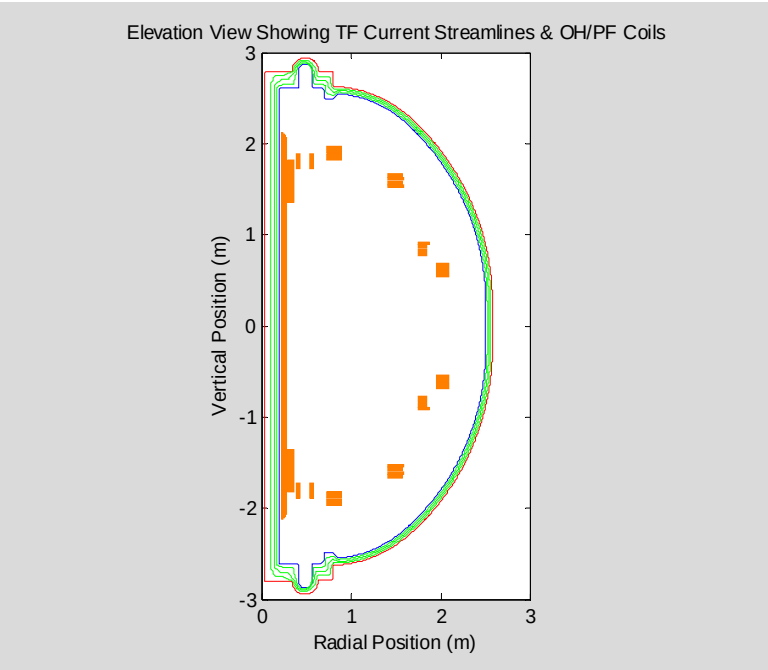

Figure 6: Poloidal Projection of PF&OH coils, with TF Current Stream Function Contours

Table 1: Assumed OH/PF Coil System

Coil Power Circuit Name	Series-connected Rectangular Winding Name	Winding Geometry				Rectangular Matrix Of Turns			conductor turn width cm	conductor turn height cm
		R (center) cm	ΔR cm	Z (center) cm	ΔZ cm	# in z direction	# in r direction	Total # turns		
OH	OH1	21.9770	1.5988	0.0000	424.1600	257	1	257	1.5988	1.6504
	OH2	23.5757	1.5988	0.0000	420.8591	255	1	255	1.5988	1.6504
	OH3	25.1745	1.5988	0.0000	417.5583	253	1	253	1.5988	1.6504
	OH4	26.7732	1.5988	0.0000	414.2574	251	1	251	1.5988	1.6504
PF1AU	PF1AU	31.9300	6.2800	159.0600	47.1000	30	4	120	1.5700	1.5700
PF1BU	PF1BU	40.0400	3.7900	180.4200	16.8300	30	6	180	0.6317	0.5610
PF1CU	PF1CU	55.0500	3.7900	180.4200	16.8300	30	6	180	0.6317	0.5610
PF2U	PF2U1	79.9998	16.2712	193.3473	6.7970	2	7	14	2.3245	3.3985
	PF2U2	79.9998	16.2712	185.2600	6.7970	2	7	14	2.3245	3.3985
PF3U	PF3U1a	148.2900	16.3100	156.9600	3.4000	1	7	7	2.3300	3.4000
	PF3U1b	149.4500	18.6400	153.5600	3.4000	1	8	8	2.3300	3.4000
	PF3U2a	148.2900	16.3100	165.0500	3.4000	1	7	7	2.3300	3.4000
	PF3U2b	149.4500	18.6400	161.6500	3.4000	1	8	8	2.3300	3.4000
PF4	PF4U1a	179.5000	9.2200	87.1100	3.4000	1	4	4	2.3050	3.4000
	PF4U1b	180.6500	11.5300	90.5100	3.4000	1	5	5	2.3060	3.4000
	PF4U2	179.4600	9.1500	80.7200	6.8000	2	4	8	2.2875	3.4000
	PF4L1a	179.5000	9.2200	-87.1100	3.4000	1	4	4	2.3050	3.4000
	PF4L1b	180.6500	11.5300	-90.5100	3.4000	1	5	5	2.3060	3.4000
	PF4L2	179.4600	9.1500	-80.7200	6.8000	2	4	8	2.2875	3.4000
PF5	PF5U1	201.2798	13.5331	65.2069	6.8580	2	6	12	2.2555	3.4290
	PF5U2	201.2798	13.5331	57.8002	6.8580	2	6	12	2.2555	3.4290
	PF5L1	201.2798	13.5331	-65.2069	6.8580	2	6	12	2.2555	3.4290
	PF5L2	201.2798	13.5331	-57.8002	6.8580	2	6	12	2.2555	3.4290
PF3L	PF3L1a	148.2900	16.3100	-156.9600	3.4000	1	7	7	2.3300	3.4000
	PF3L1b	149.4500	18.6400	-153.5600	3.4000	1	8	8	2.3300	3.4000
	PF3L2a	148.2900	16.3100	-165.0500	3.4000	1	7	7	2.3300	3.4000
	PF3L2b	149.4500	18.6400	-161.6500	3.4000	1	8	8	2.3300	3.4000
PF2L	PF2L1	79.9998	16.2712	-193.3473	6.7970	2	7	14	2.3245	3.3985
	PF2L2	79.9998	16.2712	-185.2600	6.7970	2	7	14	2.3245	3.3985
PF1CL	PF1CL	55.0500	3.7900	-180.4200	16.8300	30	6	180	0.6317	0.5610
PF1BL	PF1BL	40.0400	3.7900	-180.4200	16.8300	30	6	180	0.6317	0.5610
PF1AL	PF1AL	31.9300	6.2800	-159.0600	47.1000	30	4	120	1.5700	1.5700

Next, poloidal flux was calculated for each of the 2000 locations on each of the five contours for each of the 13 coil circuits and for a crude electromagnetic model of a "plasma" having uniform current density and a rectangular cross section extending over $0.52<r<1.63$ and $-1<z<1$, all in meters. Plots of the computed poloidal magnetic fluxes appear below in Figs.(7)-(11).

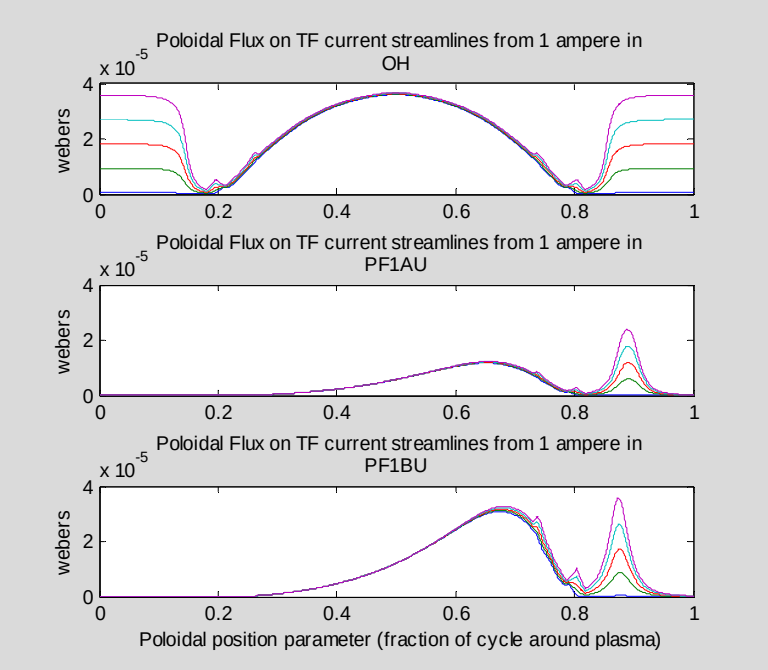

Figure 7: Poloidal Flux Per Ampere Excitation in Circuits 1-3

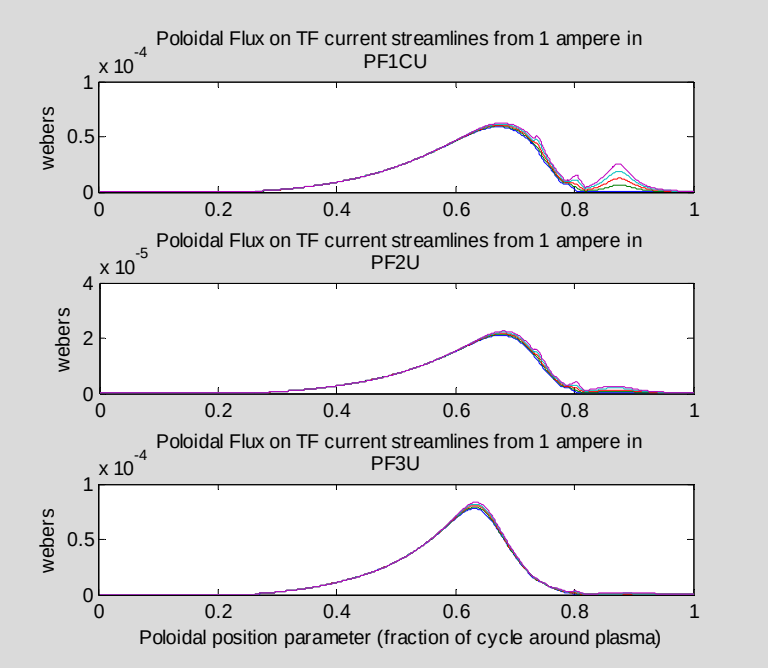

Figure 8: Poloidal Flux Per Ampere Excitation in Circuits 4-6

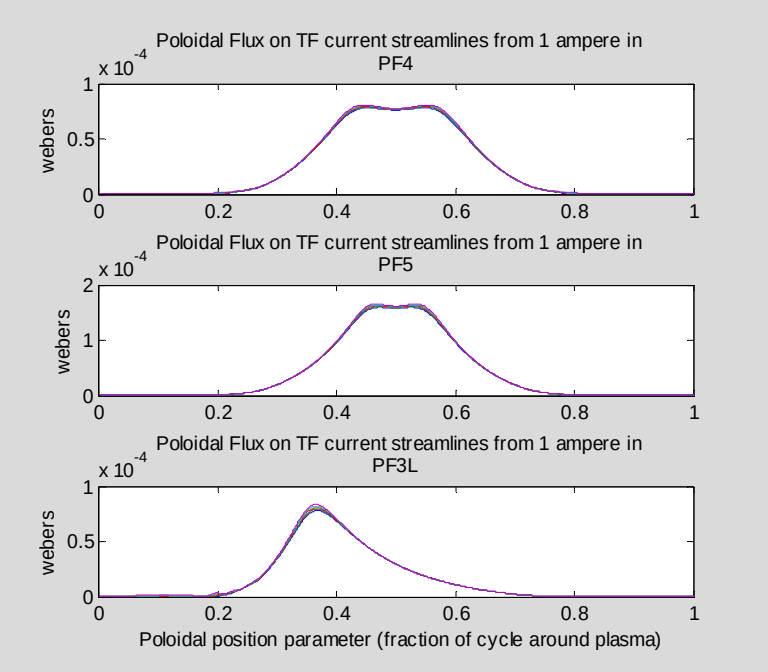

Figure 9: Poloidal Flux Per Ampere Excitation in Circuits 7-9

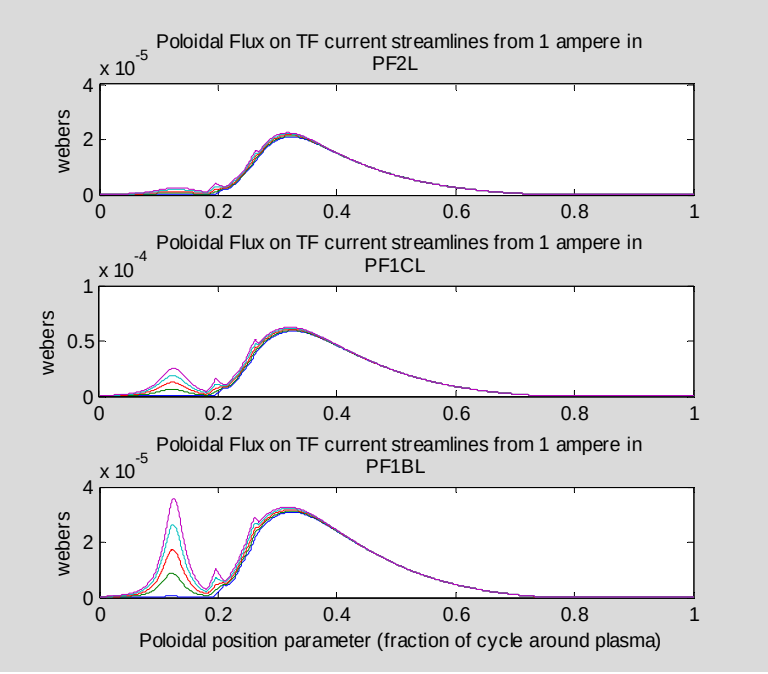

Figure 10: Poloidal Flux Per Ampere Excitation in Circuits 10-12

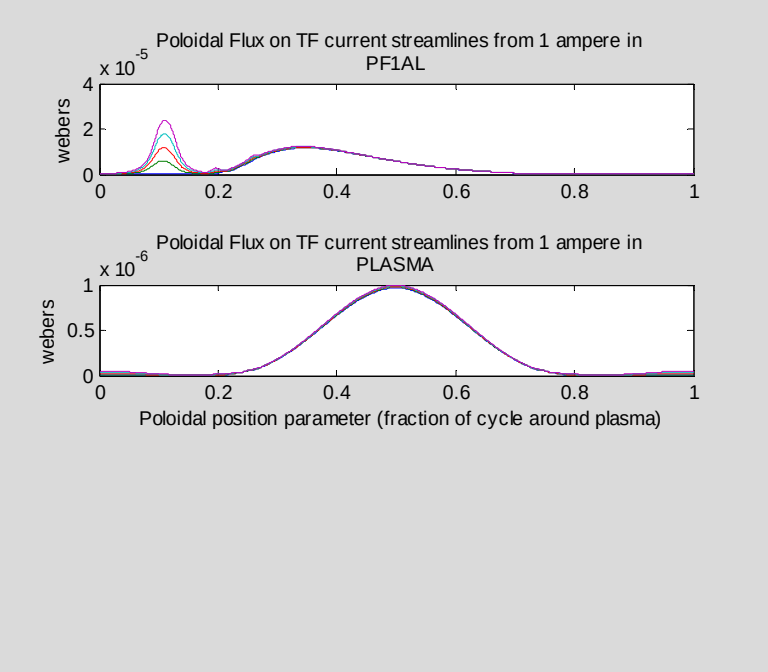

Figure 11: Poloidal Flux Per Ampere Excitation in Circuits 13-14

For each coil circuit, the mean flux was next calculated for each poloidal location as a weighted average of the flux values on the five current stream function contours, using weighting factors [0.125 0.25 0.25 0.25 0.125]. Local torque densities per ampere of circuit current are then evaluated as the product of total TF current times the finite difference derivative with respect to the poloidal angle variable of the mean flux divided by 2π. The resulting profiles were multiplied respectively by the Table 2 maximum and minimum circuit currents to establish the ranges of torque densities versus poloidal locations. Results appear in Figs.12-16.

Table 2: Assumed Coil And Plasma Current Ranges

COIL CIRCUIT NAME	MINIMUM CURRENT (Amperes)	MAXIMUM CURRENT (Amperes)
'OH'	-24000	24000
'PF1AU'	-3164.5	11049.2
'PF1BU'	-538.99	1107.333
'PF1CU'	-747.34	2053.578
'PF2U'	20000	0
'PF3U'	-16000	8000
'PF4'	-20000	15000
'PF5'	-32000	0
'PF3L'	-16000	8000
'PF2L'	20000	0
'PF1CL'	-747.34	2053.578
'PF1BL'	-538.99	1107.333
'PF1AL'	-3164.5	11049.2
'PLASMA'	0	2000000

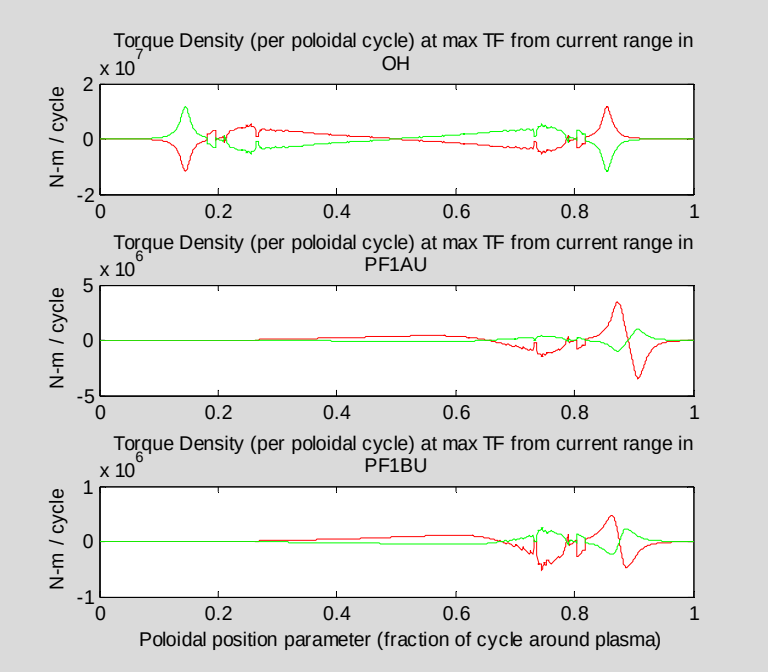

Figure 12: Torque Density For Maximal Range of Currents in Circuits 1-3

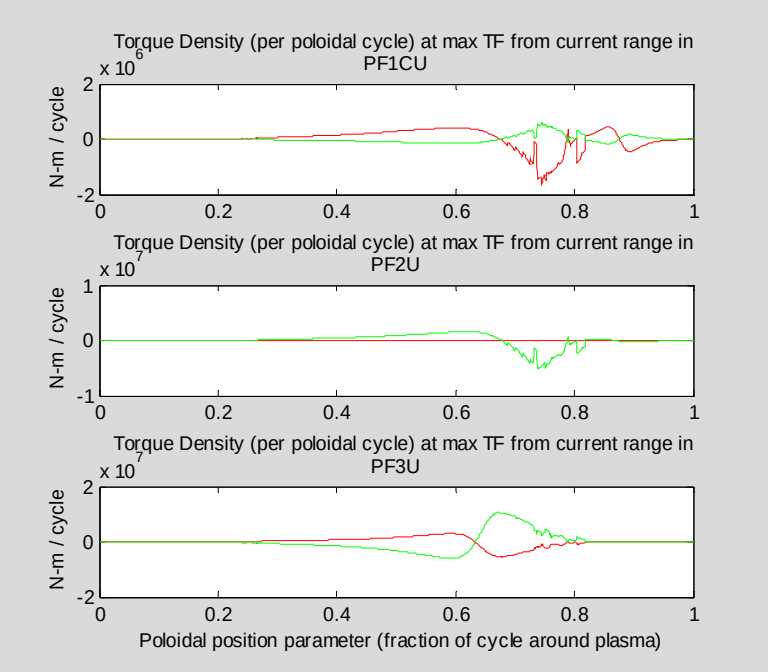

Figure 13: Torque Density For Maximal Range of Currents in Circuits 4-6

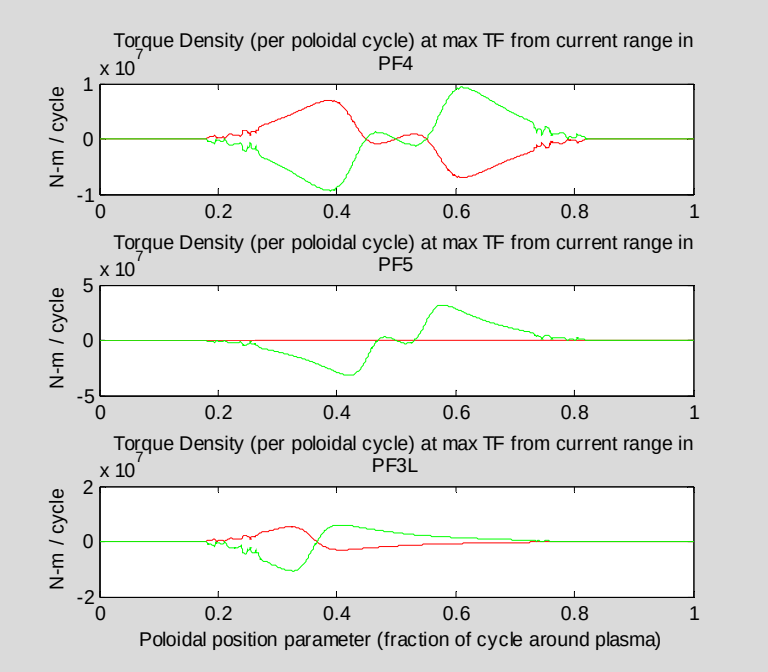

Figure 14: Torque Density For Maximal Range of Currents in Circuits 7-9

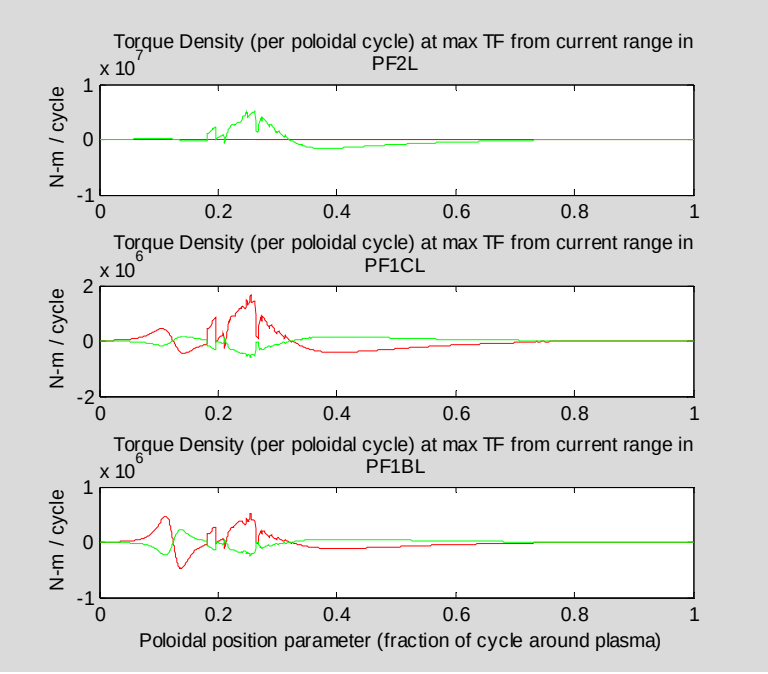

Figure 15: Torque Density For Maximal Range of Currents in Circuits 10-12

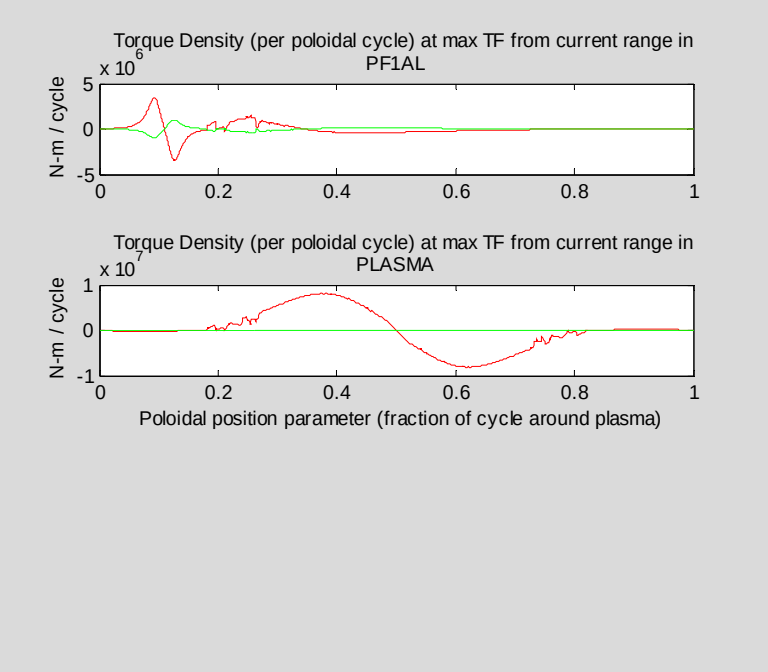

Figure 16: Torque Density For Maximal Range of Currents in Circuits 13-14

APPENDIX

Out-Of-Plane (OOP) Torque Algorithm Exposition

Derivation of Torsion Load Formulae for Out-Of-Plane (OOP) forces on Toroidal Field Coils

In general, the total moment (i.e., torque) vector of electromagnetic forces about an origin is the volume integral of the following differential:

$$d\vec{M} = \vec{r} \times \left(\vec{J} \times \vec{B}\right) dV \tag{A1}$$

where $\vec{r}$ is the position vector of a differential volume, dV, $\vec{J}$ is the current density vector and $\vec{B}$ is the magnetic field vector. For a toroidal field coil system it is appropriate to use a cylindrical coordinate system. (r,θ,z), in which the vertically oriented z axis is the central axis of symmetry which includes the origin. To analyze OOP forces in a near-axisymmetric system it is sufficient to consider only current densities and magnetic fields lying within the local poloidal plane and depending only on the position vector within that same plane. Thus, these vectors can be rewritten as follows:

$$\begin{aligned} \vec{r} &\equiv r\hat{r} + z\hat{z} \\ \vec{J} &\equiv J_r\hat{r} + J_z\hat{z} \\ \vec{B} &\equiv B_r\hat{r} + B_z\hat{z} \end{aligned} \tag{A2}$$

where $\hat{r}, \hat{\theta}, \hat{z}$ are unit vectors aligned with the local coordinate system directions.

The volume differential in cylindrical coordinates becomes:

$$dV \equiv r\, dr d\theta\, dz \tag{A3}$$

Substituting and combining terms to simplify the result, the differential moment vector is rewritten as follows in Eq. (A4)

$$d\vec{M} = \left(J_z B_r - J_r B_z\right)\left(r\hat{z} + z\hat{r}\right) r dr d\theta dz \tag{A4}$$

When integrating Eq.(A4) over the full range of toroidal angle, $0 \le \theta < 2\pi$, the radial unit vector term, $\hat{r}$, cancels itself out for rotationally symmetric poloidal magnetic fields and TF coil current densities. The remaining nonzero part of the integral is stated in Eq.(A5).

$$\vec{M} = \hat{z}\iiint \left(J_z B_r - J_r B_z\right) r^2 dr d\theta dz = \hat{z}\, 2\pi \iint \left(J_z B_r - J_r B_z\right) r^2 dr dz \tag{A5}$$

In this last form, the double integral is taken over the (r,z) poloidal half-plane. However, current density components are zero everywhere outside the TF coils so the integration region only needs to include the (r,z) projection of TF coil conductors.

An important simplification results from changing over to stream function variables. For axisymmetric systems the poloidal flux stream function, $\Psi(r,z)$, is the total magnetic flux enclosed by the circle centered on and normal to the z axis which passes through (r,z). Poloidal magnetic flux is related to the poloidal magnetic field as stated by Eq.(A6).

$$B_r(r,z) = -\frac{1}{2\pi r}\frac{d\Psi(r,z)}{dz}$$
$$B_z(r,z) = \frac{1}{2\pi r}\frac{d\Psi(r,z)}{dr} \qquad \text{(A6)}$$

so

$$\vec{B} = \frac{1}{2\pi r}\hat{\theta}\times\nabla\Psi \qquad \text{(A7)}$$

We similarly define the toroidal field coil current stream function, *I(r,z)*, as the total TF coil current enclosed by the circle about the z axis passing through (r,z). This current stream function is related to the TF current density as stated by Eq.(A8).

$$J_r(r,z) = -\frac{1}{2\pi r}\frac{dI(r,z)}{dz}$$
$$J_z(r,z) = \frac{1}{2\pi r}\frac{dI(r,z)}{dr} \qquad \text{(A8)}$$

so

$$\vec{J} = \frac{1}{2\pi r}\hat{\theta}\times\nabla I \qquad \text{(A9)}$$

Substituting these stream functions of Eqs.(A7) and (A9) into the previous integral yields Eq.(A10a).

$$\vec{M} = \iiint \vec{r}\times\left(\vec{J}\times\vec{B}\right)dV =$$
$$= \iiint \left(r\hat{r}+z\hat{z}\right)\times\left(\left(\frac{1}{2\pi r}\hat{\theta}\times\nabla I\right)\times\left(\frac{1}{2\pi r}\hat{\theta}\times\nabla\Psi\right)\right)rdrdzd\theta = \qquad \text{(A10a)}$$
$$= \frac{1}{4\pi^2}\iiint\left(\hat{z}-\frac{z}{r}\hat{r}\right)\left(\hat{\theta}\bullet\left(\nabla I\times\nabla\Psi\right)\right)drdzd\theta$$

As stated previously, the radially oriented term cancels out while integrating over toroidal angle, leaving Eq.(A10b) as the result.

$$\vec{M} = \frac{\hat{z}}{2\pi}\iint drdz\left(\frac{\partial I}{\partial r}\frac{\partial\Psi}{\partial z}-\frac{\partial I}{\partial z}\frac{\partial\Psi}{\partial r}\right) = \frac{\hat{z}}{2\pi}\iint\left(\hat{\theta}\bullet\left(\nabla I\times\nabla\Psi\right)\right)drdz \qquad \text{(A10b)}$$

This is a particularly simple and compact formula involving the integral of the cross product of gradients of two scalar functions. The poloidal magnetic flux function can be directly obtained to any desired accuracy by use of Greens functions involving the standard elliptic integral functions, K() and E(), and the current stream function can be approximated using the projected outline of TF conductors. Furthermore, the integral itself can be approximated from these data using very simple algorithms.

Limit for the case of a slender TF conductor

Vector identities applied to Eq.(A10b) imply that

$$\vec{M} = -\frac{\hat{z}}{2\pi}\iint drdz\left(\left(\nabla I \times \hat{\theta}\right)\bullet \nabla\Psi\right) \tag{A11}$$

Here, the integration is over the area of the poloidal projection of the TF conductor segment whose net torque is to be calculated. If the conductor's projection is slender with a small width, w, we can change the element of poloidal area from dA=drdz to dA=dldw where l represents distance along the conductor's length. Assuming constant current density in the conductor the gradient vector of the current stream function, ∇I , has a magnitude equal to the total TF urrent divided by the width, $\left|\nabla I\right| = \frac{I_{TF}}{w}$, and the gradient vector 's direction is perpendicular to the local TF current streamline, pointing towards the coil's bore. It follows that $\left(\nabla I \times \hat{\theta}\right)$ has the same magnitude but is pointed in the same direction as the flowing TF current, a direction denoted here by the unit vector, $\hat{n}$. With these substitutions, the net torque over a slender TF conductor segment extending from point A to point B can be rewritten as in Eq.(A12).

$$\begin{aligned}\vec{M} &= -\frac{\hat{z}}{2\pi}\iint drdz\left(\left(\nabla I \times \hat{\theta}\right)\bullet \nabla\Psi\right)\\ &= -\frac{\hat{z}}{2\pi}\frac{I_{TF}}{w}\int_0^w dw\int_A^B dl\ \hat{n}\bullet\nabla\Psi \\ &= -\frac{\hat{z}}{2\pi}I_{TF}\int_A^B dl\ \hat{n}\bullet\nabla\Psi\end{aligned} \tag{A12}$$

However, this last integral expression in Eq.(A12) may be immediately recognized as the line integral of the gradient of a scalar function, so it has the following Eq.(A13)exact solution:

$$\vec{M} = \hat{z}\ I_{TF}\ \frac{\Psi_A - \Psi_B}{2\pi} \tag{A13}$$

Thus, the general formula of Eq.(A12), when interpreted for slender conductors, asserts that the net torque over a poloidal length of TF conductor is simply the product of the difference between the poloidal flux values at the conductor's ends, divided by 2π, then multiplied by the TF current.

Derivation of Approximation For Wider TF Conductors

Consider a triangular region in the poloidal half-plane, ΔABC, on which the exact scalar functions *I(r,z)* and *Ψ(r,z)* are to be linearly approximated by $\tilde{I}(r,z)$ and $\tilde{\Psi}(r,z)$ using function values that are exact at the triangle's three corners. The linear models are as follows:

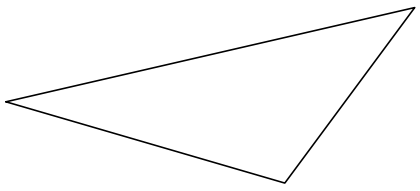

$$I(r,z) \approx \tilde{I}(r,z) = \left(\tilde{I}_0\right) + \left(\frac{\partial \tilde{I}}{\partial r}\right) r + \left(\frac{\partial \tilde{I}}{\partial z}\right) z$$
$$\Psi(r,z) \approx \tilde{\Psi}(r,z) = \left(\tilde{\Psi}_0\right) + \left(\frac{\partial \tilde{\Psi}}{\partial r}\right) r + \left(\frac{\partial \tilde{\Psi}}{\partial z}\right) z \quad \text{(A14)}$$

where $\left(\tilde{I}_0\right), \left(\frac{\partial \tilde{I}}{\partial r}\right), \left(\frac{\partial \tilde{I}}{\partial z}\right), \left(\tilde{\Psi}_0\right), \left(\frac{\partial \tilde{\Psi}}{\partial r}\right), \left(\frac{\partial \tilde{\Psi}}{\partial z}\right)$ are linear model coefficient parameters that have constant values throughout the triangle. The requirement to match the approximation to actual function values at triangle corners yields the following matrix equations, where $(r_A, z_A), (r_B, z_B), (r_C, z_C)$ are the coordinates of the triangle's corners:

$$\begin{bmatrix} 1 & r_A & z_A \\ 1 & r_B & z_B \\ 1 & r_C & z_C \end{bmatrix} \begin{bmatrix} \left(\tilde{I}_0\right) \\ \left(\frac{\partial \tilde{I}}{\partial r}\right) \\ \left(\frac{\partial \tilde{I}}{\partial z}\right) \end{bmatrix} = \begin{bmatrix} I_A \\ I_B \\ I_C \end{bmatrix} \quad \text{(A15)}$$

$$\begin{bmatrix} 1 & r_A & z_A \\ 1 & r_B & z_B \\ 1 & r_C & z_C \end{bmatrix} \begin{bmatrix} \left(\tilde{\Psi}_0\right) \\ \left(\frac{\partial \tilde{\Psi}}{\partial r}\right) \\ \left(\frac{\partial \tilde{\Psi}}{\partial z}\right) \end{bmatrix} = \begin{bmatrix} \Psi_A \\ \Psi_B \\ \Psi_C \end{bmatrix} \quad \text{(A16)}$$

These can be readily solved in closed form to find the appropriate coefficient parameter values. For the partial derivative coefficient parameters the solutions are as follows:

$$\left(\frac{\partial \tilde{I}}{\partial r}\right) = \frac{I_A(z_B - z_C) + I_B(z_C - z_A) + I_C(z_A - z_B)}{r_A(z_B - z_C) + r_B(z_C - z_A) + r_C(z_A - z_B)}$$
$$\left(\frac{\partial \tilde{I}}{\partial z}\right) = \frac{I_A(r_B - r_C) + I_B(r_C - r_A) + I_C(r_A - r_B)}{z_A(r_B - r_C) + z_B(r_C - r_A) + z_C(r_A - r_B)}$$
$$\left(\frac{\partial \tilde{\Psi}}{\partial r}\right) = \frac{\Psi_A(z_B - z_C) + \Psi_B(z_C - z_A) + \Psi_C(z_A - z_B)}{r_A(z_B - z_C) + r_B(z_C - z_A) + r_C(z_A - z_B)}$$
$$\left(\frac{\partial \tilde{\Psi}}{\partial z}\right) = \frac{\Psi_A(r_B - r_C) + \Psi_B(r_C - r_A) + \Psi_C(r_A - r_B)}{z_A(r_B - r_C) + z_B(r_C - r_A) + z_C(r_A - r_B)} \quad \text{(A17)}$$

Using this approximation the previous integrand becomes:

$$\hat{\theta}\bullet\left(\nabla I\times\nabla\Psi\right)\equiv\left(\frac{\partial I}{\partial r}\frac{\partial\Psi}{\partial z}-\frac{\partial I}{\partial z}\frac{\partial\Psi}{\partial r}\right)\approx\left(\frac{\partial\tilde{I}}{\partial r}\frac{\partial\tilde{\Psi}}{\partial z}-\frac{\partial\tilde{I}}{\partial z}\frac{\partial\tilde{\Psi}}{\partial r}\right)= \\ =\frac{I_A\left(\Psi_B-\Psi_C\right)+I_B\left(\Psi_C-\Psi_A\right)+I_C\left(\Psi_A-\Psi_B\right)}{r_A\left(z_B-z_C\right)+r_B\left(z_C-z_A\right)+r_C\left(z_A-z_B\right)} \tag{A18}$$

Note that as a result of assuming a linear model over the triangle, this approximation gives a constant value of the integrand over the triangle. Thus, the *integral* over the triangle is simply this integrand's constant value times the triangle's area, which, assuming the ABC point sequence is counterclockwise, is:

$$\left[\text{Area of Triangle }\Delta\text{ABC}\right]=\frac{1}{2}\begin{vmatrix}1 & r_A & z_A\\ 1 & r_B & z_B\\ 1 & r_C & z_C\end{vmatrix}=\frac{r_A\left(z_B-z_C\right)+r_B\left(z_C-z_A\right)+r_C\left(z_A-z_B\right)}{2} \tag{A19}$$

This cancels all (r,z) coordinates, so the integral over the triangle becomes as stated in Eq.(A20).

$$\vec{M}_{\Delta ABC}\approx\hat{z}\left(\frac{I_A\left(\Psi_B-\Psi_C\right)+I_B\left(\Psi_C-\Psi_A\right)+I_C\left(\Psi_A-\Psi_B\right)}{4\pi}\right) \tag{A20}$$

This formula can be applied to an adjacent bordering triangle, ΔACD, by changing indices as in Eq.(A21).

$$\vec{M}_{\Delta ACD}\approx\hat{z}\left(\frac{I_A\left(\Psi_C-\Psi_D\right)+I_C\left(\Psi_D-\Psi_A\right)+I_D\left(\Psi_A-\Psi_C\right)}{4\pi}\right) \tag{A21}$$

The two triangles together form a quadrilateral, ABCD, so the integral over the entire quadrilateral is the sum of the two triangle integrals:

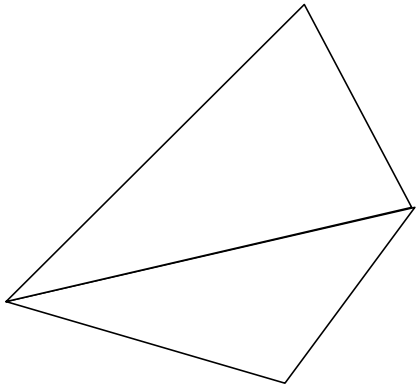

$$\vec{M}_{ABCD}=\vec{M}_{\Delta ABC}+\vec{M}_{\Delta ACD}\approx \\ \approx\hat{z}\left(\begin{array}{l}\dfrac{I_A\left(\Psi_B-\Psi_C\right)+I_B\left(\Psi_C-\Psi_A\right)+I_C\left(\Psi_A-\Psi_B\right)}{4\pi}\\ +\dfrac{I_A\left(\Psi_C-\Psi_D\right)+I_C\left(\Psi_D-\Psi_A\right)+I_D\left(\Psi_A-\Psi_C\right)}{4\pi}\end{array}\right)= \\ =\hat{z}\left(\frac{\left(I_A-I_C\right)\left(\Psi_B-\Psi_D\right)-\left(I_B-I_D\right)\left(\Psi_A-\Psi_C\right)}{4\pi}\right) \tag{A22}$$

The quadrilateral, ABCD, could alternatively be decomposed in a different way into two triangles, i.e., into triangle ΔABD and triangle ΔBCD. Although the linear coefficient parameter sets that would apply for these triangles would be different from the above, the final resulting formula for the moment integral over the quadrilateral ABCD turns out to be identically the same!

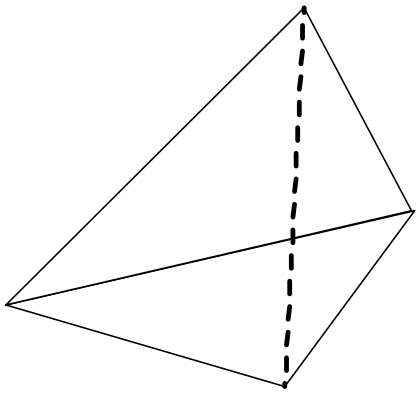

Note that in the important special case wherein the quadrilateral's corner points are located on two TF current stream function contour lines, it follows that $I_A=I_D$ and $I_B=I_C$. In that case the approximate formula for net torque in the quadrilateral region of the poloidal half-plane becomes simplified to Eq.(A23).

$$\vec{M}^{\text{AD\&BC on TFCurrent Streamlines}}_{\text{ABCD}} = \hat{z}\left(I_A - I_B\right)\left(\frac{\Psi_A + \Psi_B - \Psi_C - \Psi_D}{4\pi}\right). \qquad \text{(A23)}$$

This is the simple average of the differences between per radian poloidal magnetic fluxes at the two ends of each of the two bounding current stream function contours, multiplied by the TF current enclosed between those two current stream function contours.

Thus, the torsional OOP loading of the TF coil system can be evaluated by taking simple sums and differences of poloidal flux evaluated at points located on TF current streamlines.

A Higher Accuracy Numerical Approximation

In the present case of this memo's calculations of net torque in the NSTX CSU TF conductor due to poloidal field interactions with TF current, five TF current streamlines have been chosen and their separation in terms of contour levels is the total TF current divided by four. The adjacent diagram illustrates the five contours and flux evaluation points on those contours for two adjacent poloidal angle locations. Applying the torque formula to each of the for quadrilaterals having the ten indicated locations as their corners, the sum of the net torque is as stated in Eq.(A24).

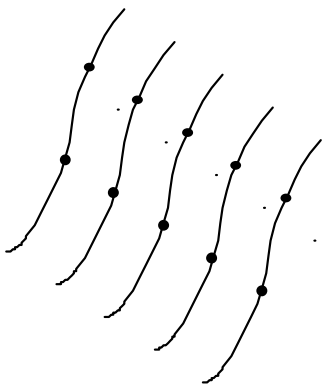

$$\begin{aligned}\vec{M} &= \hat{z}\left(\frac{I_{TF}}{4}\right)\left(\frac{\Psi_1^1 + \Psi_2^1 - \Psi_2^2 - \Psi_1^2}{4\pi}\right) + \hat{z}\left(\frac{I_{TF}}{4}\right)\left(\frac{\Psi_2^1 + \Psi_3^1 - \Psi_3^2 - \Psi_2^2}{4\pi}\right) \\ &+ \hat{z}\left(\frac{I_{TF}}{4}\right)\left(\frac{\Psi_3^1 + \Psi_4^1 - \Psi_4^2 - \Psi_3^2}{4\pi}\right) + \hat{z}\left(\frac{I_{TF}}{4}\right)\left(\frac{\Psi_4^1 + \Psi_5^1 - \Psi_5^2 - \Psi_4^2}{4\pi}\right) \qquad \text{(A24)}\end{aligned}$$

$$= \hat{z}\,\frac{I_{TF}}{2\pi}\begin{pmatrix} 0.125\left(\Psi_1^1 - \Psi_1^2\right) + 0.25\left(\Psi_2^1 - \Psi_2^2\right) + 0.25\left(\Psi_3^1 - \Psi_3^2\right) \\ + 0.25\left(\Psi_4^1 - \Psi_4^2\right) + 0.125\left(\Psi_5^1 - \Psi_5^2\right) \end{pmatrix}$$

Thus, in the sum over one poloidal interval we must premultiply the column vector of five local flux values by the row vector, [1 2 2 2 1], then divide by 16π before subtracting from the corresponding result for the other poloidal location.

Note that if all five flux values at one poloidal location were identical to each other the result would be that single value divided by 2π.

Note also that there is no benefit from repeating this summation procedure over many poloidal intervals in a TF conductor segment and summing their results, since the quantities evaluated at all intermediate poloidal locations would identically cancel each other out in taking the poloidal intervals sum. It is mathematically equivalent to directly subtract the quantities calculated on the five contours at the TF conductor segment's ends.